Electronic Supporting Information (ESI)

Multifunctional mixed-metal nanoscale coordination polymers for triple-modality imaging-guided photodynamic therapy

Yong-Mei Wang[a], Wei Liu[a], Prof. Dr Xue-Bo Yin[ab]*

[a]State Key Laboratory of Medicinal Chemical Biology and Tianjin Key Laboratory of Biosensing and Molecular Recognition, College of Chemistry, Nankai University, Tianjin, 300071, China.

[b]Collaborative Innovation Center of Chemical Science and Engineering (Tianjin), Nankai University, Tianjin, 300071, China.

*Correspondence: xbyin@nankai.edu.cn; Fax: +86-22-23503034

Table of Contents

1. Experimental Procedures

1.1 Materials

Ytterbium (III) chloride hexahydrate ($YbCl_3 \cdot 6H_2O$, 99.99%) and Tris(4,4-dicarboxylicacid-2,2-bipyridyl)ruthenium(II) dichloride Ru(II)[4,4'-$(HO_2C)_2$-bpy]$_3 \cdot Cl_2$ were obtained from Sigma–Aldrich, Shanghai, China. Gadolinium (III) chloride hexahydrate ($GdCl_3 \cdot 6H_2O$, 99.99%) and 9,10-anthracenediyl-bis (methylene) dimalonic acid (ABDA) were purchased from Aladdin Chemistry Co. Ltd., Shanghai, China. Dimethylformamide (DMF) and other solvents were from Concord Reagent Co., Tianjin, China. Ultra-pure water was prepared with an Aquapro system (18.25 MΩ). All reagents were used as purchased without further purification.

1.2 Animal Experiments

Kunming mice (~30 g), nude mice (18-25 g) and nude mice harboring HepG2 tumors in the right lateral thigh were purchased from the Institute of Hematology & Hospital of Blood Disease, Chinese Academy of Medical Sciences & Peking Union Medical College with the license No. SCXK-2014-0004, Tianjin, China. The mice access to solid rodent chow and water free. All experimental protocols using animals were approved by the Institutional Animal Care Committee of Nankai University.

1.3 Instrument and Characterization

The scanning electron microscopy (SEM) images were recorded with JSM-7500F, Japan. The transmission electron microscopy (TEM) images and EDX were recorded with Tecnai G2 F20, FEI Co. (America) operated at an accelerating voltage of 200 kV. UV-Vis absorption spectrum was recorded by a UV-2450-visible spectrophotometer (Shimadzu, Japan). The steady-state fluorescence experiments were performed on a FL-4600 Fluorescence Spectrometer (Hitachi, Japan) equipped with a plotter unit and a quartz cell (1 cm × 1 cm).

The slit width was 5 and 5 nm for excitation (460 nm) and emission, respectively. The infrared spectra were measured by the Bruker TENSOR 27 Fourier transform infrared spectroscopy. The content of Gd, Yb, and Ru was measured by Inductively Coupled Plasma Atomic Emission Spectroscopy (ICP-AES), IRIS advantage, Thermo, USA. Thermogravimetric analysis (TGA) was performed on a PTC-10ATG-DTA analyzer heated from 20°C at a ramp rate of 10°C min^{-1} under air. XRD patterns were recorded by a D/max-2500 diffractometer (Rigaku, Japan) using Cu-Kα radiation (λ = 1.5418 Å). The MR images were conducted using a MRI system (1.2 T, Huantong, Shanghai, China).

1.4 Synthesis of the single- or mixed-metal NCPs

1.4.1 Synthesis of Gd/Yb-Ru NCPs (3:0)

The mixture of $Ru[4,4'-(HO_2C)_2-bpy]_3{\cdot}Cl_2$ (**L_{Ru}**) (0.005 mmol, 4.6 mg) and $GdCl_3{\cdot}6H_2O$ (0.0065 mmol, 2.41 mg) was dissolved in 20 mL of DMF/H_2O solution containing 150 mL HCl (6 M) in a 20 mL vial. The resulting solution was heated for 2 h at 100 °C after sonication for 10 min. After cooling to room temperature, the red precipitates were collected by centrifugation at 12000 rpm for 10 min and washed twice with ethanol to afford approximately 6.1 mg of Gd/Yb-Ru NCPs 87 % yield based on **L_{Ru}**.

1.4.2 Synthesis of Gd/Yb-Ru NCPs (2:1)

The synthesis of Gd/Yb-Ru NCPs (2:1) was similar to that of Gd/Yb-Ru NCPs (3:0), with $Ru[4,4'-(HO_2C)_2-bpy]_3{\cdot}Cl_2$ (**L_{Ru}**) (0.005 mmol, 4.6 mg), $GdCl_3{\cdot}6H_2O$ (0.0043 mmol, 1.61 mg) and $YbCl_3{\cdot}6H_2O$ (0.0022 mmol, 0.84 mg). The red precipitates were isolated by washing with ethanol and dried at room temperature. Yield: 89 % based on **L_{Ru}**.

1.4.3 Synthesis of Gd/Yb-Ru NCPs (1:1)

The synthesis of Gd/Yb-Ru NCPs (1:1) was similar to that of Gd/Yb-Ru NCPs (3:0), with $Ru[4,4'-(HO_2C)_2-bpy]_3{\cdot}Cl_2$ (**L_{Ru}**) (0.005 mmol, 4.6 mg), $GdCl_3{\cdot}6H_2O$ (0.00325 mmol, 1.21 mg)

and $YbCl_3$▪$6H_2O$ (0.00325 mmol, 1.26 mg). The red precipitates were isolated by washing with ethanol and dried at room temperature. Yield: 88 % based on $\mathbf{L_{Ru}}$.

1.4.4 Synthesis of Gd/Yb-Ru NCPs (1:2)

The synthesis of Gd/Yb-Ru NCPs (1:2) was similar to that of Gd/Yb-Ru NCPs (3:0), with Ru[4,4'-$(HO_2C)_2$-bpy]$_3$▪Cl_2 ($\mathbf{L_{Ru}}$) (0.005 mmol, 4.6 mg), GdCl3▪$_6H_2O$ (0.0022 mmol, 0.80 mg) and $YbCl_3$▪$6H_2O$ (0.0043 mmol, 1.68 mg). The red precipitates were isolated by washing with ethanol and dried at room temperature. Yield: 87 % based on $\mathbf{L_{Ru}}$.

1.4.5 Synthesis of Gd/Yb-Ru NCPs (0:3)

The synthesis of Gd/Yb-Ru NCPs(0:3) was similar to that of Gd/Yb-Ru NCPs (3:0) with Ru[4,4'-$(HO_2C)_2$-bpy]$_3$▪Cl_2 ($\mathbf{L_{Ru}}$) (0.005 mmol, 4.6 mg) and $YbCl_3$▪$6H_2O$ (0.0065 mmol, 2.52 mg). The red precipitates were isolated by washing with ethanol and dried at room temperature. Yield: 89 % based on $\mathbf{L_{Ru}}$.

1.5 Cytotoxicity of PEG@NCPs

The cell viability of PEG@NCPs was tested on HepG2 cells using a standard methyl thiazolyl tetrazolium (MTT) assay. Briefly, the cells were incubated to 96-well culture plates at a density of 5 ×10^3 cells per well in culture medium. The PEG@NCPs at the concentration between 0 and 320 μg mL^{-1} were introduced to the medium and incubated 12 h after HepG2 cells reached 90-95 % confluences. As a comparison, $GdCl_3$, $YbCl_3$, and Ru[4,4'-$(HO_2C)_2$-bpy]$_3$▪Cl_2 ($\mathbf{L_{Ru}}$) at the concentration the same as that of the NCPs were added to each well. All of the cells were incubated for another 4 h. Dimethyl sulfoxide (150 μL) was used to completely liberate the formazan crystals. The absorbance at 490 nm was measured to calculate the cell viability. Three independent experiments were performed under identical conditions.

Human hepatoma carcinoma cell line (HepG2) was obtained from the Chinese Academy of Sciences (Beijing, China). HepG2 cells were maintained in complete Dulbecco's modified Eagle's medium (DMEM, Biological Industries, Israel) supplemented with 10 % fetal bovine serum (FBS, BI, Israel) and 1 % penicillin-streptomycin solution (PS, Life technologies, America). The cell lines were maintained in HERAcell VIOS 150i CO_2 incubator (Thermo scientific, America) at 37°C in a 5% CO2 atmosphere with 95% humidity. HepG2 cells (10^5 cells/mL) were dispersed within replicate 96-well microtiter plates to a total volume of 100 μl/well for MTT Assay. The plates were maintained at 37 °C in 5 % CO_2 incubator for 24 h. The cells were sequentially incubated with different concentrations of PEG@NCPs (20, 40, 80, 160, 240, and 320 □g mL^{-1} based on mass of NCPs) for 10 h. After washed three times with PBS solution, photodynamic therapy (PDT) groups were irradiated with blue LED lamp (5 W) for 10 min. Then the plates were maintained at 37 °C in 5 % CO_2 incubator for another 24 h. MTT (3-(4,5-dimethyl-2-thiazolyl)-2,5-diphenyl-2-H-tetrazolium bromide, Keygen Biotech, Jiangsu, Chian) solution (20 μL 5.0 mg/mL, BBS) was then added to each well. After 3 h, the remaining MTT solution was removed, and 150 μL dimethyl sulfoxide (Amresco, America) was added into each well to dissolve the formazan crystals. The absorbance (OD value) of each well was measured on a microplate reader (Promega, China) at the wavelength of 550 nm. Cell viability was calculated as followed:

Cell viability % = $(OD_{drug}/ OD_{control})*100\%$ (1)

For the trypan blue measurement, two different plates were used for each cell sample set; the first plate containing HeLa cells was incubated with culture; the second plate was incubated with PEG@NCPs. Both of two kinds of cells were subjected with and without LED blue light. The cells were then stained with 1 mL of 0.4 % trypan blue dye to determine the level of cell damage because the dead cells were marked with the blue color of trypan blue.

1.6 *In Vitro* fluorescent imaging with L_{Ru} or PEG@NCPs as probes

HepG2 cellls were seeded in 24-well plates at a density of 4×10^4 cells per well, the plates were maintained at 37 ° C in 5 % CO_2 air incubator for 24 h. The cells were sequentially incubated with **L_{Ru}** or PEG@NCPs (320 μg/mL) for 3 h. Then, the cells were fixed with 4 % paraformaldehyde in PBS for 20 min at room temperature, and washed with PBST (5% Tween-20 in PBS) solution three times, and the cell nuclei were stained with 4',6-diamidino-2-phenylindole (DAPI, 1 ng/mL PBS, Sigma, America) for 5 min. Confocal laser scanning microscope images of cells were captured with FV 1000 confocal microscope, Olympus, Japan. The excitation wavelengths for DAPI and NPMOFs were set at 405 nm and 480 nm, while emission was record at 425-475 nm and 570-670 nm, respectively.

1.7 Toxicity of PEG@NCPs recorded with mice as model

In vivo toxicity of PEG@NCPs was tested with mice (18−22 g, n = 3 per group) as model. After intravenous injection of the PEG@NCPs solution (20 μmol Gd^{3+} per kg), the mice anesthetized with 4 % chloral hydrate (6 mL kg^{-1}) were dissected at 7 days and all of the organs were harvested. Hematoxylin and eosin (H&E) stained images were used to investigate the difference between experimental group (injected with PEG@NCPs) and control group (injected with normal saline). The body weight of the mice was monitored with a counter balance within 28 days.

1.8 *In Vitro* MR imaging and *in vivo* fluorescence and MR imaging with PEG@NCPs

In vitro MR imaging with PEG@NCPs as probe was tested at different concentrations (0.045, 0.09, 0.18, 0.27, 0.36 and 0.45 mM) with a 1.2 T MR imaging system (Huantong, Shanghai, China). Images were obtained using a 50 mm animal coil and a fat-saturated 3D gradient echo imaging sequence. The MR imaging parameters were described as follows:

spin-echo T_1-weighted MRI sequence, TR/TE = 100.0/8.8 ms, FOV = 100 ×50 mm^2, matrix = 512 × 512, slice thickness = 1 mm, 30.0 °C.

In vivo fluorescence and MR imaging were performed on the same nude mice anesthetized with 200 μL of 4 % chloral hydrate. After intravenous injection of PEG@NCPs solution (20 μmol Gd per kg) into the mice, the fluorescence and MR profiles were obtained by positioning the mice on an animal plate in the two imaging systems. Fluorescence images were obtained on a NightOWL LB 983 small animal *in vivo* imaging system (Berthold Technologies GmbH & Co. KG, Germany) under the condition for the original emission wavelength of the PEG@NCPs (Ex = 480 nm, Em = 660 nm). The data were treated with IndiGO software.

MR imaging was performed on a 3.0 T MR imaging system (GE Signa Excite) using a small animal coil, before and at subsequent intervals following injection, using a fat-saturated 3D gradient echo imaging sequence: TR/TE = 9.7/3.0 ms; inversion time = 5.0 ms; FA = 13°; FOV = 110 mm × 110 mm; matrix = 256 × 256; slice thickness = 1 mm without gap; 176 coronal slices obtained.

1.9 *In vitro* X-ray attenuation measurement and *in vivo* CT imaging

For *in vitro* and *in vivo* CT imaging, X-ray attenuation measurement and phanton CT images were analyzed by using a clinical CT system (SIEMENS Spirit CT 31159, Germany). Parameters for the measurement and imaging were as follows: 80 kV, 210 mA; exposure time 730 ms; table speed 26.56 mm s^{-1}. Aqueous solutions of 1 mL PEG@NCPs of various concentrations as Yb at 1.04, 2.04, 3.12, 4.68, and 6.24 mg/mL were prepared for the X-ray attenuation measurement and phanton CT imaging. The attenuation values were read from the CT imaging software.

For CT imaging *in vivo*, the mice (about 22 g) were first anesthetized by intraperitoneal injection of 200 μL of 4% chloral hydrate, and then intravenously injected with PEG@NCPs solution (300 μL, 27 mg/mL). CT images were collected on the same clinical CT system with the same parameters as *in vitro* test.

1.10 *In vitro* PDT capacity investigation

$^1O_2$ generation was determined by 9,10-anthracenediyl-bi(methylene) dimalonic acid (ABDA) assay. PEG@NCPs (80 μM) was mixed with ABDA (200 μM), then the mixture was irradiated by an LED blue light (0.1 W/cm^2) lamp. The absorption of ABDA at 378 nm was monitered every five min. PEG@NCPs (80 μM) and ABDA (200 μM) at the same concentration were set as controls.

2. Results and Discussion

2.1 The preparation and validation of the mixed-metal NCPs

Before adopting simple hydrothermal method, we tried the microemulsion method because microemulsion method is often used to prepare nanoscale coordination polymers (NCPs). Sexadentate Ru(II)[4,4'-$(COOH)_2$bpy]$_3^{2+}$ ($\mathbf{L_{Ru}}$) was selected to react with Gd^{3+} ions by microemulsion method to prepare NCPs. However, we found the morphology and size of the NCPs were almost unaffected by the content of surfactant. Uniform Gd-Ru NCP spheres were also obtained by heating the mixture of $\mathbf{L_{Ru}}$ and Gd^{3+} ions in DMF/H_2O system without any auxiliary ligand or surfactant (Fig. 1a). Therefore, we adopted simple hydrothermal strategy for the preparation of NCPs and proposed the self-limiting growth mechanism.

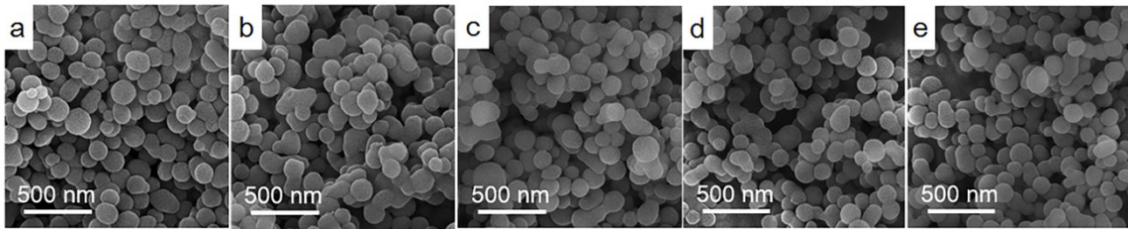

Fig. S1 SEM images of Gd/Yb-Ru NCPs with different Gd^{3+}/Yb^{3+} ratio. (a) 3:0, (b) 0:3, (c) 2:1, (d) 1:1, (e) 1:2.

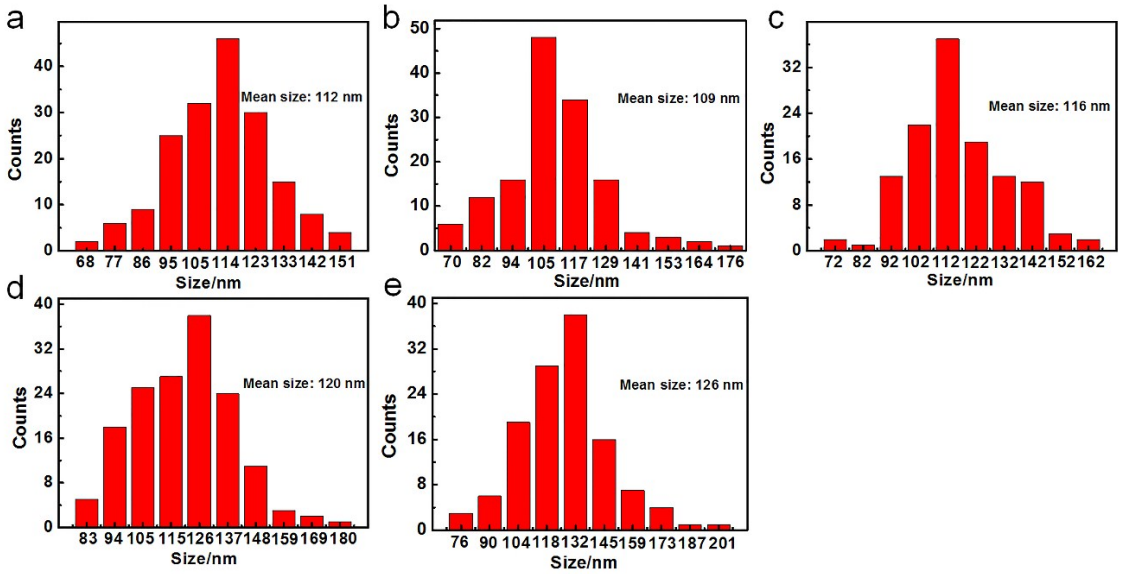

Fig. S2 Size distrition ontainted from SEM images of Gd/Yb-Ru NCPs with Ln^{3+} ratios of (a) 3:0, (b) 0:3, (c) 2:1, (d) 1:1, and (e) 1:2.

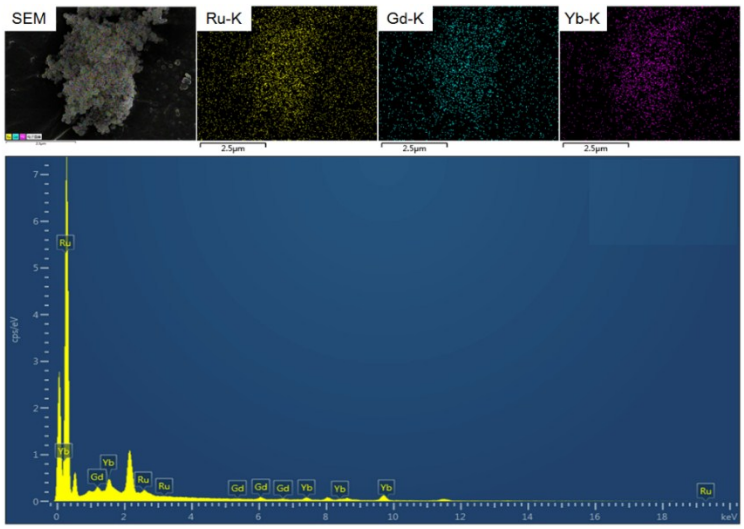

Fig. S3 EDS elemental mapping of the Gd/Yb-Ru NCPs with Gd^{3+}/Yb^{3+} ratio of 1:1.

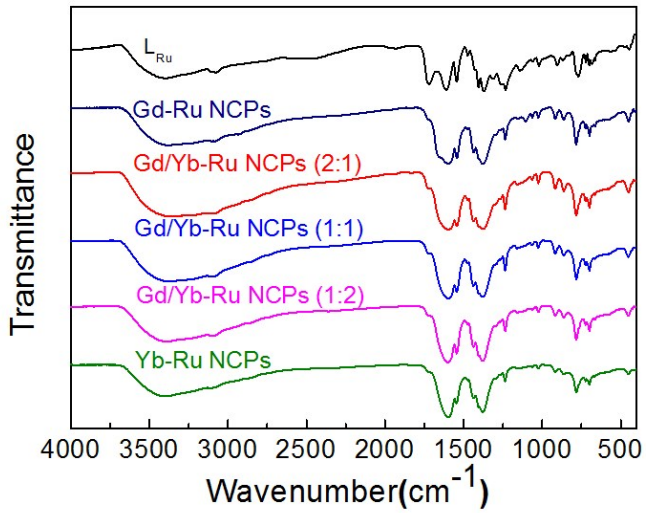

Fig. S4 Infrared spectra of Gd/Yb-Ru NCPs with the Gd/Yb ratios of 2:1, 1:1, 1:2, 0:3, and $\mathbf{L_{Ru}}$.

In the IR spectra of $\mathbf{L_{Ru}}$ and NCPs (Fig. S4), the broad peak centered at 3392 cm^{-1} is attributed to O-H stretching vibrations of uncoordinated carboxyl groups on the surface, residual water and ethanol. The strong band at 3076 cm^{-1} in both $\mathbf{L_{Ru}}$ and the NCPs is attributed to the =C-H stretching vibrations of the pyridine rings.[1] The strong band centered at 1720 cm^{-1} in $\mathbf{L_{Ru}}$ arises from the stretching vibrations of C=O bond,[2] while the band at 1720 cm^{-1} blue shifted to 1630 cm^{-1} in the NCPs, demonstrating the coordination of -COOH with Gd^{3+}. The stretching vibrations of C=N bond at 1543 cm^{-1} from the pyridine rings of are observable in $\mathbf{L_{Ru}}$ and the NCPs.[1]

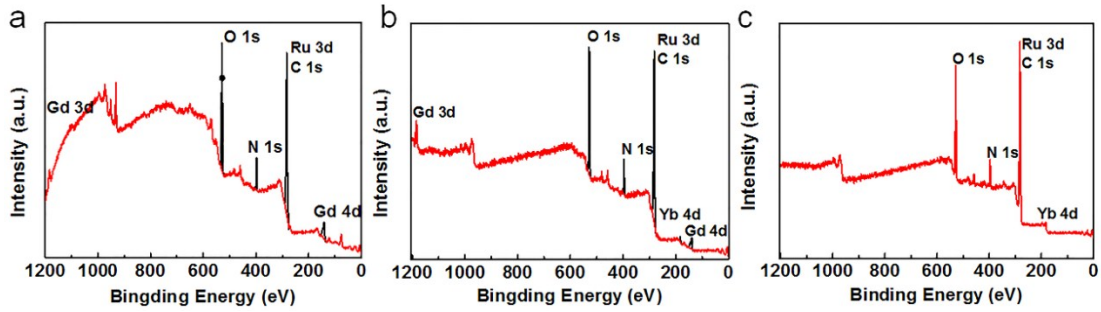

Fig. S5 X-ray photoelectron spectroscopy (XPS) patterns of Gd/Yb-Ru NCPs with Ln^{3+} ratios of (a) 3:0, (b) 1:1, and (c) 0:3.

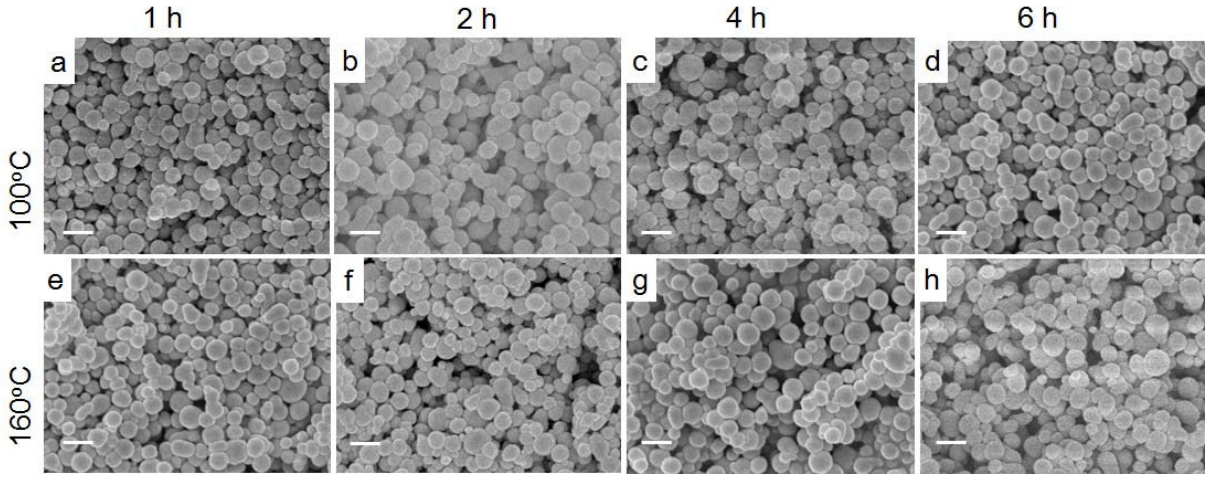

Fig. S6 SEM images of the NCPs synthesized at (a-d) 100 and (e-h) 160 °C for 1-6 h. Scale bars = 200 nm.

2.2 Validation of the high yield of the mixed-metal NCPs

Gd^{3+}, Yb^{3+} and $\mathbf{L_{Ru}}$ can be dissolved in DMF/H_2O/HCl mixture solvent to form uniform solution as illustrated in Fig. S7a. Aftere reaction, the mixture solution was subjected to centrifuge. A clear supernatant was obtained (Fig. S7b). Thus, 100 % of $\mathbf{L_{Ru}}$ was integrated into the NCPs. After simple centrifugation and washing with ethanol/H_2O of the NCPs, the yields, which were calculated based on $\mathbf{L_{Ru}}$, were all higher than 85% with the simple and robust procedure.

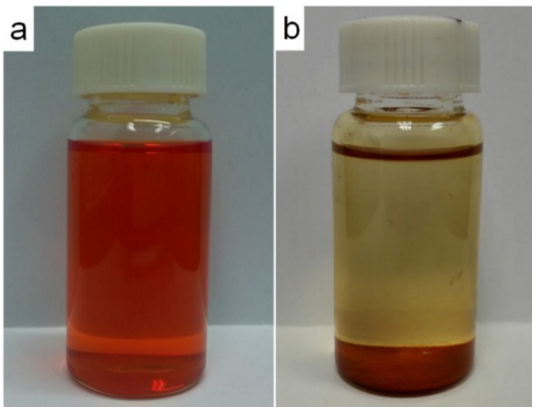

Fig. S7 The images of the mixture solution of Gd^{3+}, Yb^{3+}, and $\mathbf{L_{Ru}}$ (a) before and (b) after heating at 100 °C for 2 h for the preparation of the mixed-metal NCPs.

2.3 Self-limiting growth of the mixed-metal NCPs

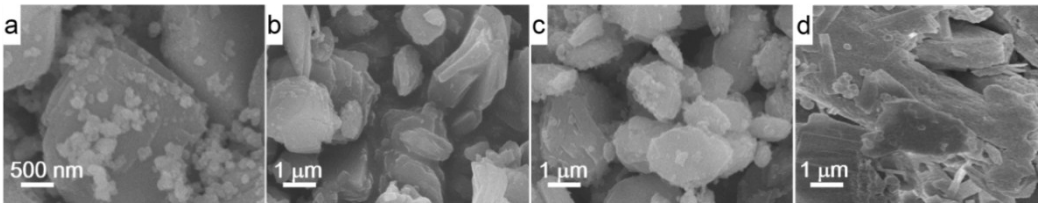

Fig. S8 SEM images of the products results from $\mathbf{L_{Ru}}$ and (a) Fe^{2+}, (b) Zn^{2+}, (c) Mn^{2+}, and (d) Gd^{3+} and [Ru(II)(4,4'-COOH-bpy)$_2$bpy].

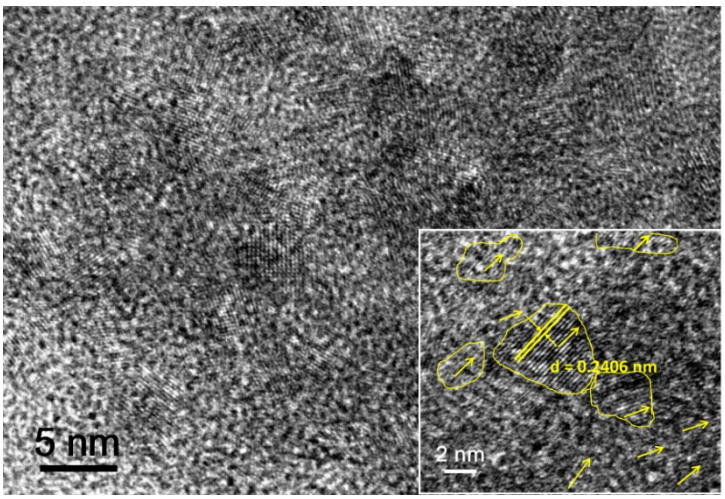

Fig. S9 High-resolution TEM image of the Gd/Yb-Ru NCPs sphere; lattice fringes are highlighted in yellow.

Powder X-ray diffraction (XRD) of the NCPs did not exhibit well defined diffraction peaks (Fig. S10), but the broad peak centered at 22° indicate partly crystal structure.[3,4] No obvious difference in reflection peak angle was observed despite the different Gd/Yb ratios in those NCPs. The broad peak centered at 22° confirmed that the NCPs are amorphous structurally. Although crystal islands were observed, their different orientation led to the total amorphous structure of the NCPs.

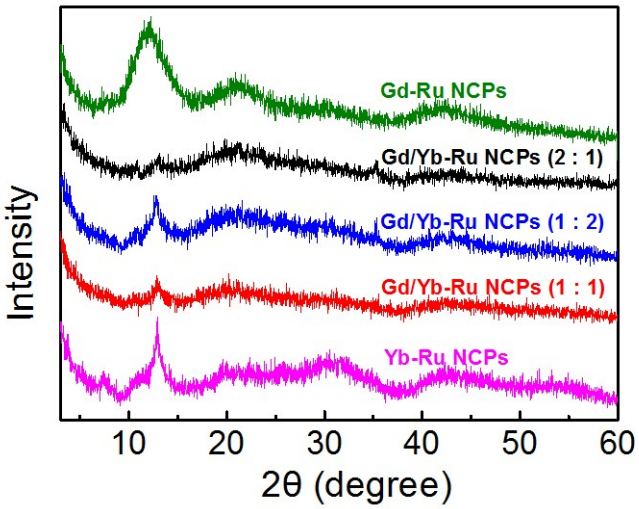

Fig. S10 PXRD patterns of Gd/Yb-Ru NCPs synthesized with the Gd/Yb ratios of 3:0, 2:1, 1:1, 1:2, and 0:3.

2.4 Composition of the mixed-metal NCPs

Table S1. Ru/Gd/Yb molar ratios in precursors, and obtained from elemental mapping and ICP-AES results of Gd/Yb-Ru NCPs (3:0), Gd/Yb-Ru NCPs (2:1), Gd/Yb-Ru NCPs (1:1), Gd/Yb-Ru NCPs (1:2), and Gd/Yb-Ru NCPs (0:3).

Sample	In precursors	In elemental mapping	In ICP-AES results
Gd/Yb-Ru NCPs (3:0)	1:1.30:0	1:1.34:0	1:1.32:0
Gd/Yb-Ru NCPs (2:1)	1:0.87:0.43	--	1:0.83:0.44
Gd/Yb-Ru NCPs (1:1)	1:0.65:0.65	1:0.65:0.64	1:0.62:0.65
Gd/Yb-Ru NCPs (1:2)	1:0.43:0.87	--	1:0.41:0.83
Gd/Yb-Ru NCPs (0:3)	1:0:1.30	1:0:1.24	1:0:1.20

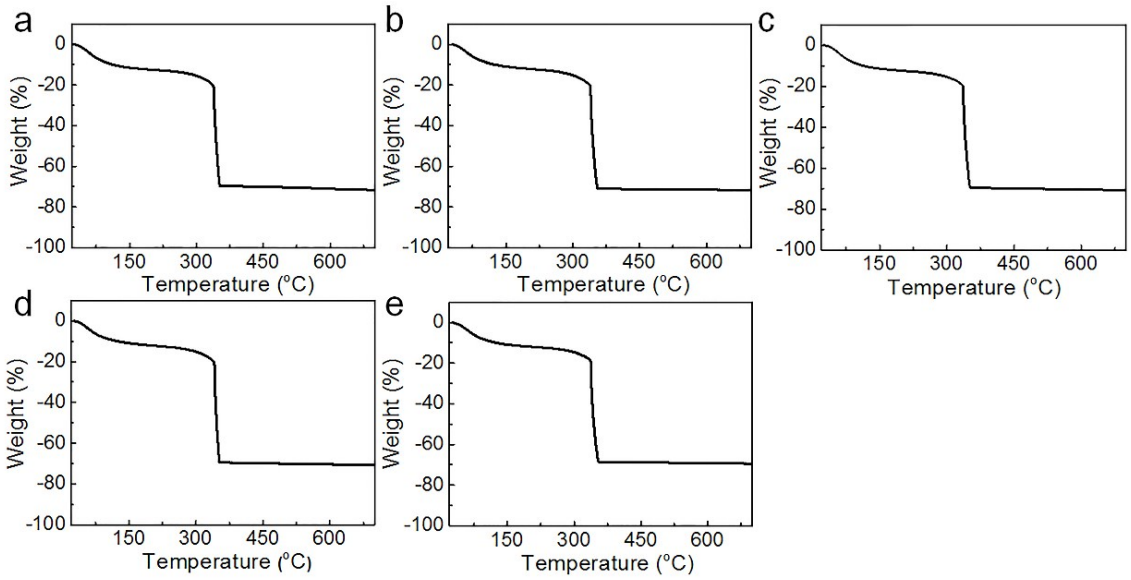

Fig. S11 Thermogravimetric analysis (TGA) of Gd/Yb-Ru NCPs with Ln^{3+} ratios of (a) 3:0, (b) 2:1, (c) 1:1, (d) 1:2, and (e) 0:3.

Table S2. Comparison of C, N, and H content found in elemental analysis and calculated results of Gd/Yb-Ru NCPs (3:0), Gd/Yb-Ru NCPs (2:1), Gd/Yb-Ru NCPs (1:1), Gd/Yb-Ru NCPs (1:2), and Gd/Yb-Ru NCPs (0:3).

Sample	Found (%)			Calculated (%)[a]		
	C	N	H	C	N	H
Gd/Yb-Ru NCPs (3:0)	37.59	7.47	2.89	37.91	8.15	2.42
Gd/Yb-Ru NCPs (2:1)	37.17	7.32	2.51	37.61	8.09	2.41
Gd/Yb-Ru NCPs (1:1)	37.12	7.22	2.98	37.49	8.07	2.40
Gd/Yb-Ru NCPs (1:2)	36.83	7.29	2.48	37.34	8.04	2.369
Gd/Yb-Ru NCPs (0:3)	36.65	7.26	2.96	37.06	7.98	2.37

[a] The calculated formula of the NCPs with Gd/Yb ratios of 3:0, 2:1, 1:1, 1:2, and 0:3 were $\mathbf{L_{Ru}}Gd_{1.3}\cdot 7H_2O$, $\mathbf{L_{Ru}}Gd_{0.85}Yb_{0.45}\cdot 7H_2O$, $\mathbf{L_{Ru}}Gd_{0.65}Yb_{0.65}\cdot 7H_2O$, $\mathbf{L_{Ru}}Gd_{0.45}Yb_{0.85}\cdot 7H_2O$, and $\mathbf{L_{Ru}}Yb_{1.3}\cdot 7H_2O$, respectively.

2.5 Optical properties of the mixed-metal NCPs

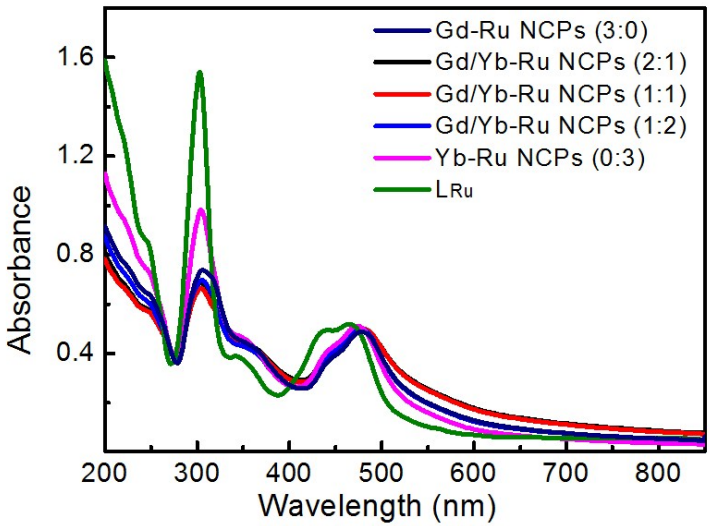

Fig. S12 UV-vis absorption of L_{Ru} and Gd/Yb-Ru NCPs with the Gd/Yb ratios of 3:0, 2:1, 1:1, 1:2, and 0:3.

2.6 Stability, cytotoxicity, and high biocompatibility of PEG@NCPs

After the same pretreatment with Gd/Yb-Ru NCPs, the TGA analysis of PEG@NCPs was carried out (Fig. S13). The appearance of decomposition curve (380 ^{o}C) of PEG proves its successful coating, and the grafted amount is about 13%.

The stability of PEG@NCPs was tested to validate their practicability. To investigate the stability of the PEG@NCPs, the NCPs were dissolved in saline solution containing 10 % fetal bovine serum (FBS) at 37 ^{o}C. After different time intervals, 1 mL aliquots of the solution were used for TEM examination (Fig. S14). The size and morphology of PEG@NCPs remained unchanged over 24 h, illustrating their chemical stability (Fig. S14).

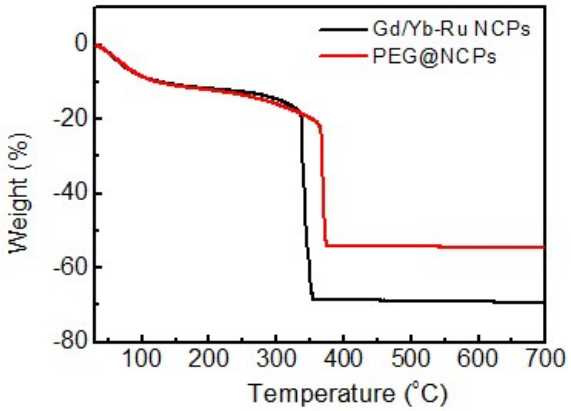

Fig. S13 Thermogravimetric analysis (TGA) of PEG@NCPs. The PEG@NCPs was obtained by mixing 4 mL of NCPs (1 mg mL^{-1}) solution with 1 mL PEG6000 (4 mg mL^{-1}) and stirring for 5 h at 60°C.

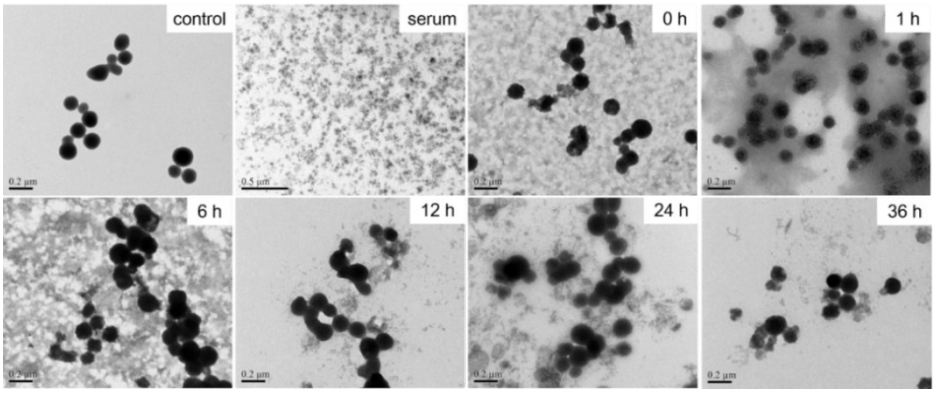

Fig. S14 TEM images of serum only and PEG@NCPs incubated in water (control) and in saline supplemented with 10% fetal bovine serium for diffferent time.

2.7 Triple-modality imaging and biodistribution of PEG@NCPs

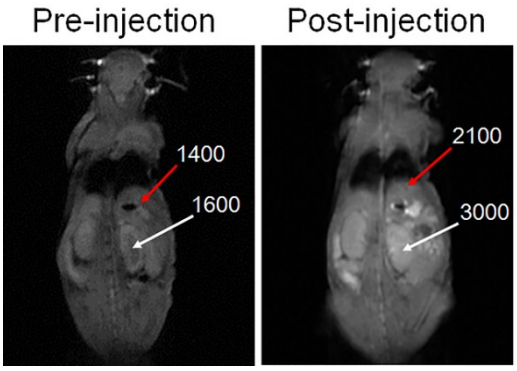

Fig. S15 MR images of nude mice with PEG@NCPs as probe. White and red arrows indicate kidney and liver, respectively.

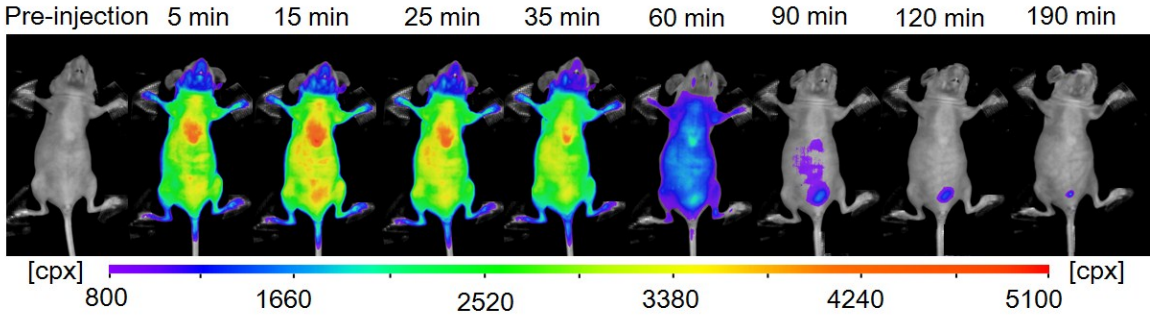

Fig. S16 In vivo fluorescence imaging of the mice after the injection of PEG@NCPs (20 μmol Gd^{3+} per kg).

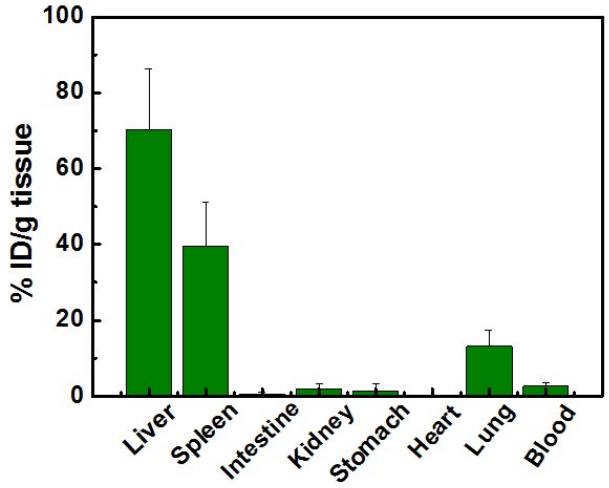

Fig. S17 The Yb content in the dissected organs and blood samples.

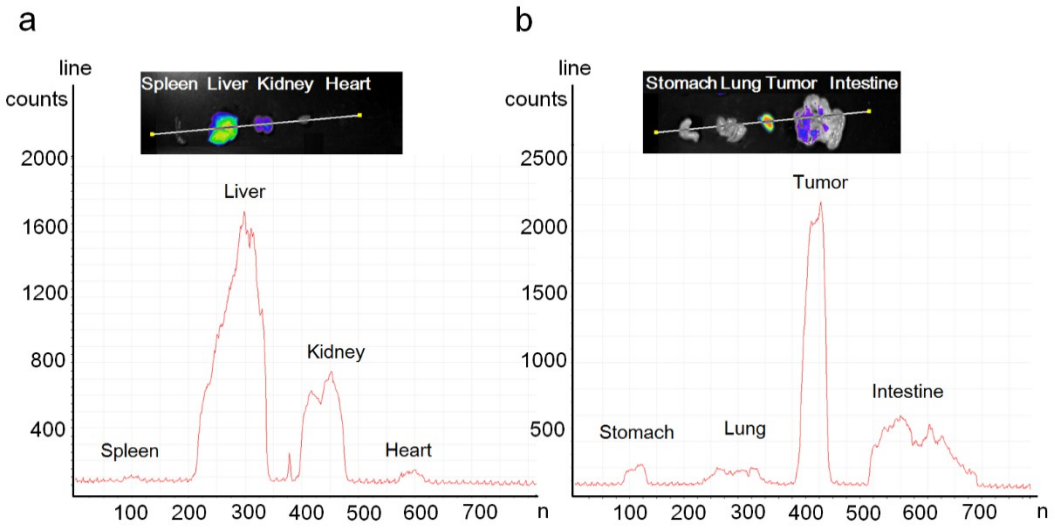

Fig. S18 The fluorescence signal intensity across the line in the panel of different organs dissected from the tumor-bearing mouse. (a) spleen, liver, kidney, and heart, (b) stomach, lung, tumor, and intestine.

2.8 singlet oxygen generation and PDT capacity of PEG@NCPs

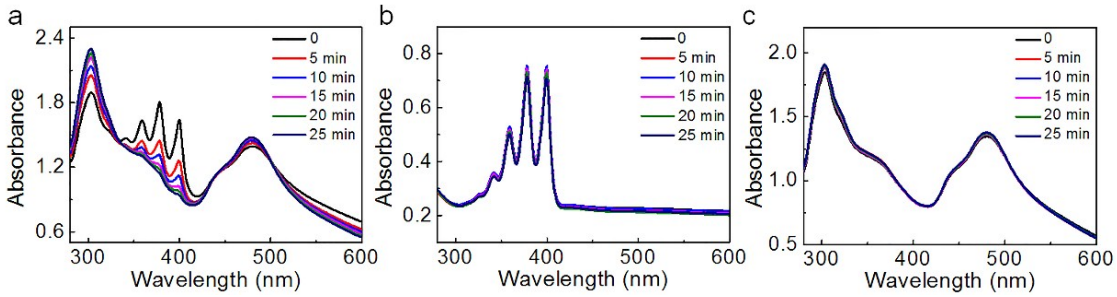

Fig. S19 UV-vis absorption spectra for the photobleaching of (a) 200 μM ABDA for monitering of $^1O_2$ after mixted with 80 μM PEG@NCPs; (b) control groups of 200 μM ABDA and (c) 80 μM PEG@NCPs with the irradiation over a period of 25 min.

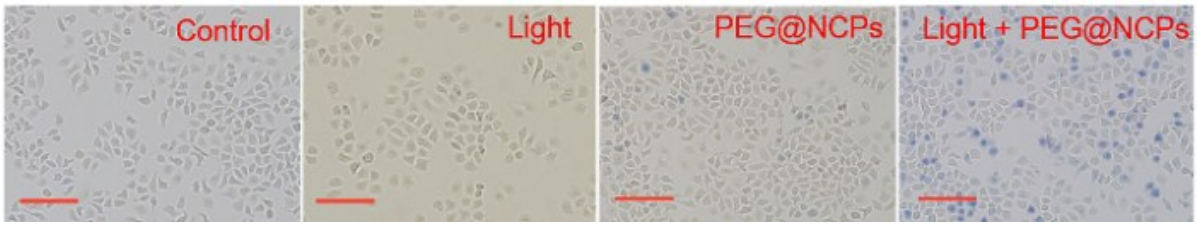

Fig. S20 CLSM images of HepG2 cells after incubation of PEG@NCPs with and without excitation of 480 nm for 10 min. The dead cells were marked by trypan blue. Scale bars: 200 μm.

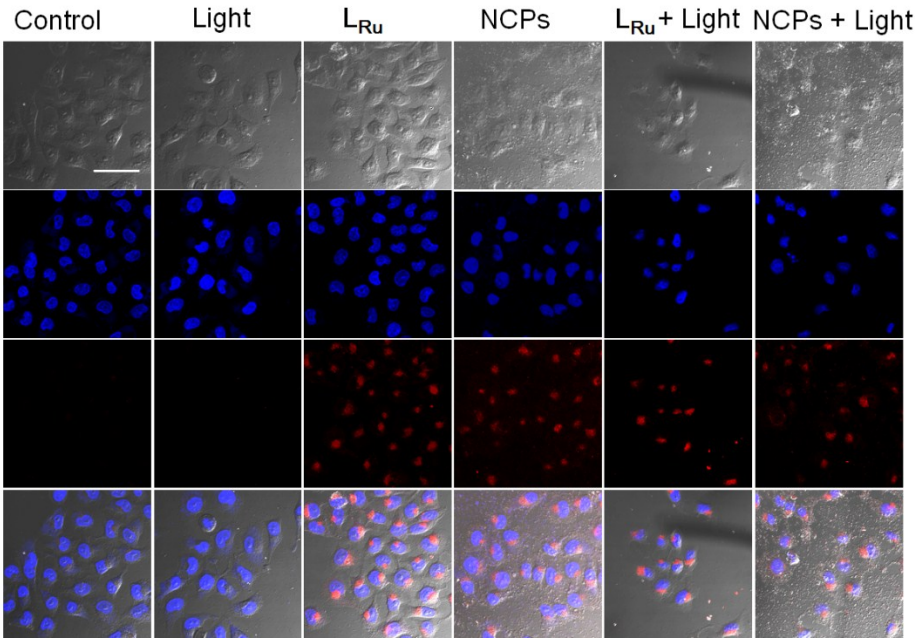

Fig. S21 CLSM images of HepG2 cells incubated with $\mathbf{L_{Ru}}$ or PEG@NCPs for 3 h. Scale bar: 100 μm.

3. References

1 J. Yang, C. Li, Z. Quan, C. Zhang, P. Yang, Y. Li, C. Yu, J. Lin, *J. Phy. Chem. C 2008*, **112**, 12777-12785.

2 Y. Zhou, X. Li, L. Zhang, Y. Guo, Z. Shi, *Inorg. Chem. 2014*, **53**, 3362-3370.

3 T. D. Bennett, A. K Cheetham,. *Acc. Chem. Res. 2014*, **47**, 1555-1562;

4 Zhang, Z. Nguyen, H. T. H. Miller, S. A. Cohen, S. M. *Angew. Chem. Int. Ed. 2015*, **54**, 6152-6157.